Single-nuclei RNA-seq on human retinal tissue provides improved transcriptome profiling.

Qingnan Liang[1, 2, 3]*, Rachayata Dharmat[1]*, Leah Owen[4], Akbar Shakoor[4], Yumei Li[1], Sangbae Kim[1], Albert Vitale[4], Ivana Kim[4], Denise Morgan[4, 5], Nathaniel Wu[1], Margaret DeAngelis[4]#, Rui Chen[1, 3]#

* Equal contributions.

Corresponding authors. Margaret DeAngelis, margaret.deangelis@utah.edu; Rui Chen, ruichen@bcm.edu

[1]HGSC, Department of Molecular and Human Genetics, Baylor College of Medicine, Houston, TX, 77030, United States.

[2]Biochemistry and Molecular Biology Graduate Program, Baylor College of Medicine, Houston, TX, 77030, United States.

[3]Verna and Marrs McLean Department of Biochemistry and Molecular Biology, Baylor College of Medicine, Houston, TX, 77030, United States.

[4]Department of Ophthalmology and Visual Sciences, University of Utah, Salt Lake City, UT, 84132, United States.

[5]Department of Pharmacotherapy, the College of Pharmacy, University of Utah, Salt Lake City, UT, 84132, United States.

ABSTRACT

The retina is the innermost layer of tissue in the eyes of human and most other vertebrates. It receives the information of the visual images like the film of a camera, translates the images into neural signals, and transduces the signal to the brain. Three layers of neural cells (photoreceptor cells, bipolar cells, and ganglion cells) within the retina are comprised of seven major cell types; rod, cone, Müller glia cell, amacrine cell, horizontal cell, bipolar cell, and retinal ganglion cells, which create visual perception through functional cooperation. In all retinal diseases, it is the ultimate degeneration of the photoreceptors, the rods and cones, which results in blindness. Understanding all the individual cell types and how they contribute the basic neural circuitry in both the human and mouse retina will be key to elucidating mechanism of retinal degenerations.

Here, we report to the best of our knowledge the first single-nuclei RNA-seq based transcriptomic study on human neural retinal tissue. We sequenced 6544 nuclei from six samples, and 4730 nuclei passed the quality filtering steps. The donor samples came from both the macular and peripheral regions, respectively, from three donors' retina. None of the donors had any evidence of any ocular disease including retinal diseases as evidenced by medical record and post mortem imaging and phenotyping (Owen et al., IOVS in press). Unsupervised clustering was able to identify all seven cell populations. Known markers of neural retinal cell types were used to assign the clusters to these seven major retinal cell types, and thus, gene expression profiles for each cell type were obtained. With this dataset, the similarities and differences in cell proportion and gene expression between human and mouse were assessed. We highlighted the genes that demonstrated statistically significant differential distribution between human and mouse photoreceptors. In addition, the gene expression profiles of the same cell types between the macular and peripheral regions between human and mouse were compared. Specifically, as a means of validation the highly expressed genes in photoreceptor cells were found to be significantly enriched in known inherited retinal disease genes. Thus, we propose that this cell-specific gene list would serve as a prioritization during not only novel disease gene discovery, but cell-specific pathway gene analysis. This should

facilitate a better understanding of retinal cell biology with the goal of cell-specific therapeutic interventions for retinal degenerations, as therapies are limited.

INTRODUCTION

The transduction of visual signals occurs in a highly specialized tissue of the central nervous system called the retina. The retina is derived from the neuroectoderm and the specialization stems from the underlying complexity from the diverse cell types[1,2]. In the human retina this is an ordered array of approximately 70 different types of neurons across 5 major classes: photoreceptor (rods and cones), retinal ganglion cells (RGCs), horizontal (HC), bipolar (BPC), amacrine (AC) along with a non-neuronal muller glial cell (MG), each playing a unique role in processing the visual signal[3,4]. This neuronal cell type classification has been traditionally defined based on morphological, connectional and functional characteristics[4]. Only recently, with the advent of robust and scalable single cell-RNA profiling have we been able to explore the cellular heterogeneity based on a quantifiable molecular feature- the cellular transcriptome[5–7]. Analysis of the transcriptome at the single cell level, allows the discovery of novel cell types (including subtypes of bipolar, amacrine, and RGCs)[6–8], identification of cell-type specific genetic markers, and most importantly, gives a snap-shot view of the cellular function of rare cell types unique to human and/or mouse retina.

These extensive cell type characterizations have thus far been limited to the mouse retina[6–8]. Mouse models can serve as an exceptional model for dissection of genetics and physiology of cellular function in the mammalian retina. However, the mouse retina lacks certain features unique to the retina of humans and simian primates, most importantly the macula[9,10]. The macula is a central depressed region (that subtends an angle of ~20 degrees) in the human retina[11]. It further encompasses a 1.5mm central region which includes an avascular pit comprised of long- and medium-wavelength (L/M) cone photoreceptors and a few short-wavelength (S) cones, but no rods[11]. This unique distribution is essential both for high visual acuity and color vision perception in the retina. The macula is responsible for central vision and is necessary for reading, recognition of faces, and driving. The macula is surrounded by a region in the retina that is highly enriched in rods constituting the peripheral retina that is functionally crucial for dim light and peripheral vision[11]. These differences are not solely architectural, but also have unique differentiation and downstream cellular connections indicating a distinct functional and thus transcriptional profile of cells in the central vs the peripheral region[11–13]. The differences between the macular and periphery has not yet been investigated at a single-cell transcriptomic level.

In addition to the macular region, mouse studies are also inadequate for representing the human-like cone profile. For example, L-cones are only limited to human and other primates and not in mouse. To date, no human adult cone profiles have been reported and this is largely due to the low proportion of cones in human retina (compared to other retinal cell types) and the difficulty in sorting cones from rods. As indicated previously, cones are functionally important[4,14–16]. Retinal degenerations, including, cone-rod dystrophy (CRD) which generally affects cone cells first, are usually early onsite (childhood) and yet uncurable[17,18]. With the hope of gene therapy moving into early clinical phases, targeting different genes it is imperative to understand the human cone gene expression profiles. Moreover, this would also aid for retinal diseases characterized by other cell types such as rods for retinitis pigmentosa (RP) and/or RGCs for glaucoma[19–24]. Thus, understanding the transcriptional variance across cell types of the human retina would facilitate translational research.

In this study we use single nuclei-RNA seq, here in referred to Nuc-seq which is an improvement over the standard single cell-RNA seq especially for neuronal tissue[25–28]. This technique overcomes the issue of transcriptional perturbation as an artifact of cellular dissociation protocols. Importantly, Nuc-seq gives an accurate representation of the cellular transcriptome of the low levels of mRNA contained in the nucleus of the cell that otherwise would be understudied by standard single cell-seq protocols[28]. As a result, Nuc-seq can be successfully applied on frozen tissue samples. We performed Nuc-seq on both the peripheral and macular region of 3 human donor retina samples to profile 4730 nuclei. Through unsupervised clustering of the gene expression profiles, 7 clusters could be identified, and they matched the 7 major cell types in human retina (rod, cone, MG, HC, AM, BC, and RGC). We compared the photoreceptor profiles between human and reported mouse profiles and assessed the similarities and differences between the profiles. Moreover, we compared the gene expression profile between macular and peripheral region, both as an entity and by individual cell type. With the differentially expressed genes (DEGs) identified, we found that photoreceptor DEGs significantly enriched inherited retinal disease (IRD) genes, indicating that the photoreceptor DEG lists would facilitate prioritization for novel disease gene discovery and cell-specific pathway analysis. Overall, this should facilitate a better understanding of retinal cell biology with the goal of cell-specific therapeutic interventions for retinal degenerations, as therapies are currently limited.

MATERIALS AND METHODS:

Macular and peripheral sample collection

As previously described in detail (Owen et al., in press) human donor eyes were obtained in collaboration with the Utah Lions Eye Bank. Briefly, only eyes within 6 hours postmortem time were used for this study. Both eyes of the donor undergo rigorous post mortem phenotyping including spectral domain optical coherence tomography (SD-OCT) and color fundus photography. Most importantly these images are taken in a manner consistent with the appearance of the analogous images utilized in the clinical setting. Dissections of donor eyes were carried out immediately according to a standardized protocol to reliably isolate the RPE/choroid from the retina and segregate the layers into quadrants[29] (Owen et al., in press). After the eye is flowered and all imaging is complete, macula retina tissue is collected using an 6mm disposable biopsy punch (Integra, Cat # 33-37) centered over the fovea and flash frozen and stored at -80°C. The peripheral retina is collected in a similar manner from each of the four quadrants. To determine the precise ocular phenotype relative to disease and or healthy aging, analysis of each set of images is performed by a team of retinal specialists and ophthalmologists at the University of

Utah School of Medicine, Moran Eye Center and the Massachusetts Eye and Ear Infirmary Retina Service. Specifically, each donor eye is phenotyped by independent review of the color fundus and OCT imaging; discrepancies are resolved by collaboration between a *minimum* of 3 specialists to ensure a robust and rigorous phenotypic analysis. This diagnosis is then compared to medical record and a standardized epidemiological questionnaire for the donor. For this study both eyes for each donor were classified as AREDS 0/1 to be considered normal. Only one eye was used for each donor. Donors with any history of retinal degeneration, diabetes, macular degeneration, or drusen, were not used for this study. Institutional approval for consent of patients to donate their eyes was obtained from the University of Utah and conformed to the tenets of the Declaration of Helsinki. All retinal tissues were de-identified in accordance with HIPPA Privacy Rules.

Preparation of single-nucleus suspensions

Nuclei from frozen neural retinal tissue was isolated using RNase-free lysis buffer (10 mM Tris-HCl, 10 mM NaCl, 3 mM MgCl2, 0.1% NP40). The frozen tissue was resuspended in ice cold lysis buffer and triturated to break the tissue structure. The tissue aggregates were then homogenized using a Wheaton™ Dounce Tissue Grinder and centrifuged (500g) to pellet the nuclei. The pellet was re-suspended in fresh lysis buffer and homogenized to yield clean single-nuclei suspension. The collected nuclei were stained with DAPI (4',6-diamidino-2-phenylindole, 10ug/ml) and were diluted to 1000 µl of 3E4/ml with 1× PBS (without Ca++ and Mg++, pH 7.4, Thermo Fisher), RNase inhibitor (NEB, 40KU/ml) and Cell Diluent Buffer.

The ICELL8™ single cell based single cell capture

Single nuclear capture and sequencing was performed on the ICELL8 single cell platform (Wafergen Biosytems). ICELL8 platform comprises of a multi-sample nano-dispenser that precisely dispensed 50nl of the single nuclei suspension into an ICELL8 nanowell microchip containing 5184 wells (150nl capacity). Assuming a Poisson distribution frequency for the number of cells per well, about 30% of the nanowells were expected to contain a single-nuclei under optimal conditions. Automated scanning fluorescent microscopy of the microchip was performed, using Olympus BX43 fluorescent microscope with a robotic stage, to visualize wells containing single nuclei (see Table 1 for single cell capture number across different experimental repeats). Automated well selection was performed using the CellSelect software (Wafergen Biosystems) which identified nanowells containing single nuclei, and excluded wells with >1 nuclear, debris, nuclei clumps or empty wells. The candidate wells were manually evaluated for debris or clumps as an additional QC.

Single-cell RT-PCR and library preparation

The chip was subjected to freeze-thaw in order to lyse the cells and 50 nl of reverse transcription and amplification solution (following ICELL8 protocol) was dispensed using the multi-sample nano-dispenser to candidate wells. Each well has a preprinted primer that contains an 11 nucleotide well-specific barcode which is added to the 3’ (A)n RNA tail of the nuclear transcripts during reverse transcription and CDNA amplification performed on candidate wells using SCRB-seq chemistry. After RT, the CDNA products from candidate wells were pooled, concentrated (Zymo Clean and Concentrator kit, Zymogen) and purified using 0.6x AMPure XP beads. A 3’ transcriptome enriched library was made by using Nextera XT Kit and 3’-specific P5 primer which was sequenced on Illumina Hiseq2500.

Data analysis

For bulk RNA-seq, FASTQ sequences were mapped to human genome hg19 (GRCh37) downloaded from UCSC genome browser website and aligned using STAR[30]. Transcript structure and abundance were estimated using Cufflinks[31–34].

For single-cell RNA-seq data analysis, FASTQ files were generated from Illumina base call files using bcl2fastq2 conversion software (v2.17). Sequence reads were aligned to the human genome hg19 (GRCh37). For transcriptome analysis, aligned reads were counted within exons using HTseq-count using default parameters[35]. All genes that were not detected in at least 2.5% of all our single cells were discarded for all further analyses. Cells were filtered based on a minimum number of 500 expressed genes per cell, a minimum number of 6000 and a maximum number of 100000 transcripts per cell. Data were log-transformed [log(read count + 1)] and normalized for all downstream analyses, using Seurat package (http://satijalab.org/seurat/)[36]. MultiCCA method in Seurat was used to align all the six datasets (3 macular, 3 peripheral). Aligned data were used for single cell clustering, tSNE visualization and differentially expressed gene (DEG) analysis. DEGs were assigned following three criteria: first, at least 25% of the very population expressed this gene; second, the gene in the very group should pass Wilcoxon rank sum test against the reference group with Bonferroni adjusted p-value<0.05; third, the average fold-change of the gene in the very group against the reference group is more than 1.28 (logFC>0.25). Functional enrichment analysis was performed using DAVID[37].

For mouse single-cell RNA-seq, the expression data was obtained from GSE63473[7]. Matrices from seven P14 mice, GSM1626793-1626799, were used for analysis. Gene filter of detection in >1% cell and cell filter of gene expression number over 500 were applied. CCA alignment and DEG analysis were performed with a similar procedure as the human sample.

RESULTS

Generation and the quality evaluation of the human retinal tissue single-nuclei RNA-seq.

To generate transcriptome profiles for human photoreceptor cells, specially cones, retinae from three individual separate healthy donors were obtained (n = 3 donors). All three donors are Caucasian male and range from 60 to 80 years and were phenotyped as normal as described in methods. There is no visible pathogenic indication, not even macular drusen, a hallmark of age-related macular degeneration, commonly found in this age group, according to the fundus images[38]. As previously described, two sample punches from each retina (n =6), one from the macula region and the other from the peripheral region, were subjected for single cell nuclei RNA-Seq. After dispensing, nano-wells were imaged and wells with single nuclei were selected. cDNA library construction and sequencing were performed for a total of 6544 individual nuclei. Distribution of the number of nuclei from each sample is listed in Table 2. To exclude low quality data, several QC steps are conducted (detailed in methods). As results, 1,814 nuclei are filtered out due to poor quality, leaving a total number of 4730 nuclei for downstream analysis. On average, 31783 mapped reads are obtained per nucleus with the median number of genes detected at 1054. To further evaluate the quality of snRNA-Seq data, bulk RNA-seq from the corresponding sample was performed. Good correlation between the bulk gene expression (FPKM) and single-nuclei gene expression (average of normalized read count) was observed with positive correlation coefficient ranges from 0.57 to 0.72. Thus, to the best of our knowledge, we report the first single-nuclei RNA-seq analysis on human retinal tissue.

Unbiased single-cell transcriptomics profiling identifies all seven neuronal cell types of human retina.

To identify individual retinal cell types, we performed unbiased clustering on the gene expression profiles of 4730 human retinal nuclei. Seven clusters are identified, each of which contains cells from all six samples (Figure 1A), suggesting relatively low sample bias. Based on the expression pattern of cell type specific marker genes in the cluster, it is possible to map each cluster to individual cell types (Figure 1C). As shown in Figure 1B, markers for known retinal cell types, such as PDE6A for rod cells, TRPM1 for bipolar cells (BC), SLC1A3 for Muller glial cells (MG), GAD1 for amacrine cells (AM), SEPT4 for horizontal cells (HC), ARR3 for cone cells and RBPMS for retinal ganglion cells (RGC), show cluster specific expression pattern. Thus, each cluster could be assigned to a known retinal cell type, which is further supported by examining additional known marker genes for each cell type (Supplement Table 1). A total of 122, 96, 126, 211, 228, 299 and 396 differentially expressed genes (DEGs) are identified for rod, BC, MG, AM, HC, cone, and

RGC cell respectively (Supplement Table 2). Gene ontology enrichment analysis of biological process terms were performed with these DEGs (Supplement Table 3).

Similarities and differences in cell proportion between human and mouse retina are revealed.

Based on the number of nuclei in each cluster, we were able to quantify the proportion of each cell type in the sample. As shown in Fig 2D-E, composition of different cell types from human peripheral retina was generally consistent with that from previous mouse studies, with the exception of a higher percentage of MG cells and a lower percentage of AM cells being observed in the human retina. This trend is consistent with the results reported from a previous study in monkey[39], in which relative ratio of BC: MG: AC: HC is close to 4:3:2:1. As expected, a lower rod proportion and higher BC, HC and RGC proportions are observed in the human macular sample compared with the human peripheral retina. Thus, our study reveals the similarities and variances of retinal cell proportions between human and mouse retina.

DEG analysis reveals human rod-cone differences.

More than 60% of the retina cell population is composed of photoreceptor cells. By combining rod and cone photoreceptor cells, a list of 147 genes that are highly enriched in photoreceptors was obtained (Supplement Table 2). These genes show significant enrichment of biological process GO terms of visual perception, rhodopsin mediated signaling pathway, maintenance of photoreceptor cells and regulation of rhodopsin mediated signaling pathway (Figure 2A). This is largely consistent with the known function of photoreceptor cells, which further validate our cluster assignment and DEG analysis.
Although both cell types are photoreceptor cells, there are important differences between rod and cone cells, including, their cell shape, spatial distribution in retina, and role in the phototransduction pathway. Rod cells are responsible for dim light vision with low spatial acuity, while cone cells are responsible for color vision with higher spatial acuity. While this is largely because rod and cone share a similar phototransduction mechanism, the

genes involved are different members of the same family. As a result, knowledge gained form studying rods cannot always be translated to our understanding of cone cells. Through transcriptome comparison between rods and cones, we demonstrated 22 genes that have a higher expression in rod cells and 276 genes that have a higher expression in cone cells (Supplement table 4). Interestingly, GO analysis indicates that the visual perception term is highly enriched in both gene sets (Figure 2B-C, Supplement Table 4). Most of these genes are known rod and cone markers. For example, GNAT1, PDE6A, NR2E3, PDE6G, CNGA1, SAG, ROM1, RHO are highly enriched in rods while GUCA1B, GUCA1C, OPN1LW, PDE6H, CNGB3, GNAT2, RD3, PDE6C, ARR3 etc. are highly expressed in cones. Differentially enriched GO terms by the two set of genes include rhodopsin mediated signaling pathway and regulation of rhodopsin pathway for rod highly expressed genes and response to stimulus, sodium ion membrane transport, and cilium assembly for cone highly expressed genes. These genes may provide us with new angles in distinguishing rod and cone cells.

Genes with different rod cone distributions between mice and humans were revealed.

Mice, the most studied animal model for retinal degeneration, are not an ideal model for studying cone biology as its cones have significant differences from those in humans. For example, in the human retina, cone cells are highly enriched in a region called the fovea near the central macula which is absent in the mouse retina[9,40]. In addition, mice have two types of cone-opsins, namely Opn1sw for short-wavelength sensing and Opn1mw for middle- and long-wavelength sensing. Some mouse cone cells express only one type of opsin while a considerable proportion (40% for C57/BL6 mice) express both[41]. In contrast, humans have three types of cone-opsins, OPN1SW, OPN1MW and OPN1LW, and each cone cell only express one type of opsin[16]. 383 and 343 DEGs of mouse rods and cones were obtained from the published single-cell RNA-seq data of mouse retina by using very similar analyses methods (Supplement Table 5). These genes were compared with the 122 and 299 human rod and cone DEGs and showed considerable overlap (Figure 2D). Of note, we found 19 genes as both mouse rod and cone DEGs, but only as human cone

DEGs (Supplement Table 5), indicating that mouse models might not be that suitable for this set of genes. Two of these genes, RPGRIP1 and RD3, appears as known human IRD genes[42–51] and show high expression in human cone cells, compared with rod cells (Figure 2E). Patients with mutations in RPGRIP1 and RD3 were reported with LCA and CRD, which showed a more severe cone phenotype than rod. In contrast, KO mouse models of these two genes are reported to display RP phenotypes[51–53], which were mostly resulting from rod issues. Thus, we demonstrated that mouse models of specific retinal degeneration associated genes do not faithfully recapitulate the human condition.

Differentially expressed genes in the macular region compared with peripheral region.

The macula is a structure unique to human and other primates. Although the macular region and the peripheral share the same types of cell, we demonstrate that the proportion of cell types are different between macular and peripheral human retina (Figure 1 D-E). We first examined the overall differentially expressed genes between the macular and peripheral region. We found 200 genes that are highly expressed in the macular region and 172 genes that are highly expressed in the peripheral region (Supplement Table 6). The macular genes enrich the microtubule skeleton organization, microtubule-based process, substantia nigra development etc GO terms (Figure 6A-B), indicating a more neuronal-like transcriptome, while the peripheral genes are enriched for visual perception and rhodopsin related signal transduction pathways. This indicates that the result of overall comparison is largely driven by the differences in cell proportions. Using a SAGE approach, Sharon et al reported 20 genes with higher expression in the macula and 23 genes with higher expression in peripheral region, in the retina[13]. 9 macular genes (NEFL, STMN2, UCHL1, NDRG4, TUBA1B, DPYSL2, APP, YWHAH, MDH1) and 14 peripheral genes (SAG, RCVRN, UNC119, RHO, GPX3, PDE6G, ROM1, TF, ABCA4, DDC, PDE6B, GNB1, GNGT1, NRL) are consistent with our data. Li et al reported 1239 genes with higher expression in macular retina and 812 genes with higher expression in the peripheral macular region[12]. Full gene lists were not reported for comparison while the enriched GO terms, such as ion transport in macular genes and visual perception in peripheral genes (Figure 3A-B), demonstrate similarity.

Our snRNA-Seq data allows the comparison of gene expression between macular and peripheral retina for the same cell type in well characterized fresh donor eye tissue. Correlation of averaged gene expression patterns of five cell types, rod, cone, MG, BC and AM, from each sample were calculated (Figure 3C). HC and RGC are not assessed here limited by the small number of cells found in the peripheral region. For these cell types, the profiles across six samples show reasonable high correlation with each other while the macular ones showing even higher correlations, which indicates that some differences do exist within the cell types according to the cell location. We then tested whether some of the DEGs of these cell types show uneven expression in the macular and peripheral region. Among the DEGs, 75 rod DEGs, 3 cone DEGs, 44 MG DEGs, 10 BC DEGs and no AM DEGs show different distribution between the macular and peripheral region (Supplement Table 6).

Differentially expressed genes in photoreceptor cells enrich inherited retinal disease genes.

With the expression profile for each retinal neuronal cell type generated in this study, we sought to examine its potential utility in identifying genes associated with human retina diseases. A gene list of 234 genes that contains all the known IRD genes for RP, LCA, CRD, and other retinopathies was obtained from the retnet (RetNet, http://www.sph.uth.tmc.edu/RetNet/) (Supplement Table 7). As expected, robust expression of most of these known IRD genes (197 of the 234) could be detected in our dataset (Supplement Table 7). Additionally, the detected IRD genes are expressed at significantly higher level than average (Figure 4A, p-value = 2.27e-07, two-sample t-test). Since the vast majority of known IRD associated genes affects photoreceptor cells exclusively, we reason that significant overlap should be detected between IRD genes and the photoreceptor enriched gene set. Indeed, 44 IRD genes are among the 147 PR DEGs, representing a 16-fold enrichment over background (p-value<2.2e-16, fisher's exact test) (Figure 4B, Supplement Table 8). Depending on the timing and severity of rod and cone photoreceptors defect, IRDs can be classified into different subtypes clinically. For example, although cone photoreceptor cell degeneration is observed as the disease progresses, RP is primarily due to defect in rod photoreceptors[54–56]. On the other hand, cone-rod dystrophy (CRD) is result from cone degeneration from the very beginning[17,18]. Among the 44 IRD genes that show photoreceptor cell-specific expression, 26 have been associated with RP while 11 have been associated with CRD. Consistent with the clinical phenotype, on average, RP associated genes have higher expression in rod cells while CRD associated genes show higher in cone cells (Figure 4C-D).

Given the significant enrichment of IRD associated genes in the cell type DEG set, it can be potentially used to prioritize candidate IRD disease genes. To test this idea, the eye phenotype for mice with photoreceptor cell DEG orthologous gene mutated is examined. For the 103 photoreceptor DEGs that have not been associated with human retina diseases, 49 have knock out mice recorded in the MGI database with non-lethal phenotypes. Among them, 18 shown phenotypes in the visual system (Supplement Table 8), such as GNGT1, RDH8 and RCVRN. Protein encoded by GNGT1 is known to locate in the outer segment of photoreceptor cells and plays important role in phototransduction[57,58]. RDH8 gene encodes a human retinol dehydrogenase, and mutation of its mouse ortholog causes delayed rod function recovery after light exposure and accumulation of all-trans-retinal in the rod outer segment[59]. RCVRN is a calcium binding protein which is a regulator of rod sensitivity of dim lights, and it is also found to be an auto-antigen of cancer-associated retinopathy[60]. Thus, our photoreceptor cell DEG list would serve as a prioritization tool for novel disease gene discovery, with the genes with reported mouse eye phenotype being the high priority ones.

Retinal disease genes and mouse phenotype related genes in other retinal cell types.

In contrast to the significant overlap between IRD genes and photoreceptor (PR) DEGs, no significant enrichment is observed in DEGs for other retina cell types. It has been shown that defects in cell types in the neural retina other than PR can also lead to IRD. Indeed, 14 known IRD genes show enriched expression in cell types not restricted to photoreceptor cells (Supplement Table 8). From those genes, we found a few of them have known functions consistent with the expression pattern and human phenotype. For example, RDH11 is highly expressed in Muller Glia cell which plays an important function in retinal cycle and mutations in RDH11 lead to RP[61]. GRM6 and TRPM1 are bipolar DEGs and their mutations could cause congenital stationary night blindness (CSNB) in a recessive mode, while CSNB is known to be caused by abnormal photoreceptor-bipolar signaling[62–68]. Besides, in there DEG lists, 28, 30, 38, 32, and 18 genes that are highly expressed in MG, HC, RGC, AM and BC, respectively, showed correlation to the mouse eye phenotypes (Supplement Table 8). These genes could potentially serve as prioritization for further study of non-PR-related IRDs.

DISCUSSION

Here, we report the transcriptome profiles of the human retinal major cell types at the single- nuclei level from 4730 cells. Unsupervised clustering identified seven clusters which could be assigned to the seven major retinal cell types: rod, cone, MG, BC, AM, HC and RGC. We extracted transcriptomic signatures from each cluster, which provide an invaluable resource for researchers

The utility of single-nuclei RNA-seq on human retinal tissue is also assessed in our study. Single-nuclei RNA-seq is a viable alternative method to single-cell RNA-seq which is more practical for human tissue study because it could be applied to frozen neuronal tissue. Gao et al reported that in breast cancer cells the single-nuclei RNA-seq was representative of single-cell RNA-seq[69]. Our single-nuclei profiles showed good correlation with bulk RNA-seq of the same sample, and the cell type profiles also displayed consistency with published human retinal cell markers. Additionally, we found that floating mRNA could be a resource of contamination among cell types as a limitation of this approach, although this limitation did not affect our study on the major cell types. We found 299 highly expressed genes in human cones and looked for differences between human rods and cones. Currently, cone cells are much less studied than rod cells. This is because: first, the human cone cells are more different from mouse cone cells compared with the differences between their rods; and second, in human, there are about 20-fold more rods and lastly, the retina is a neural tissue and it is it is challenging to separate rods and cones by current experimental approaches. Mustafi et al previously compared the transcriptomes between cone-enriched macular region and rod-enriched peripheral region in monkey to analyze rod and cone signatures[70]. They found known cone makers, SLC24A2 and OPN1MW and the RGC genes, including, NEFL and NEFM, which were driven by the uneven proportion of RGCs in the macular and peripheral region. Welby et al developed a sorting method to enrich fetal cones in human and studied the transcriptome[71]. Their findings demonstrated the cone signature during the development (9 to 20 weeks post conception), which could be useful in recapitulating some aspects of the human adult cone. Our study took advantage of “in silico” sorting to separate cones from other cell types and thus provided better profiling. With an improved cone profile, we also highlighted a few genes which show different distribution in photoreceptor cells between human and mouse. For example, two genes, RD3 and RPGRIP1, showed elevated expression in human cones compared to rods, while they showed similar expression level in mouse cones and rods. The expression level in human tissue of these two genes were consistent with the immunohistochemical data in the human protein atlas (www.proteinatlas.org), and pathogenic phenotype in human patients (LCA and CRD). Another improvement in our study is concerning the macular profiles. The macula is a region in the central retina that looks yellow under fundus imaging which is known to be responsible for accute vision and color vision. Diseases causing macula damage, such as age-related macular degeneration (AMD) or Stargadts, cause loss of central vision which is usually more severe compared with loss of peripheral vision. The Mouse retina does not possess such a structure, and although some AMD disease models were reported, they could only recapitulate aspects of the human phenotype[9]. Thus, the similarities of the gene expression profiles of each of the cell types in macular and peripheral regions of the retina remained unknown. Here we reported that the same types of cells in the macular region have a higher correlation with each other compared with the periphery. We also reported multiple DEGs between the macular and peripheral region both overall and within each of the cell types. The functional relationships between the genes and the region still require more study.

With the highly expressed genes found, we further examined these gene lists from the perspective of inherited retinal diseases, including RP, LCA, cone-rod dystrophy etc. Generally, the early onset of these diseases is within one single cell type, and then gradually affect others. Significant enrichment of IRD genes in our photoreceptor DEGs was detected compared with DEG lists of all other cell types. Thus, we propose that the rest of the list would serve as a powerful tool for gene prioritization in disease gene discovery and pathway analysis.

Author Contributions:

RC and MD conceived the project. QL, SK, RD and NW did the data analysis. LO, AS, AV, IK, DM and MD collected the human donor retinas, performed the phenotyping and dissection. RD and YL prepared the nuclei sample and performed the single-nuclei RNA-seq. QL, RD, MD and RC wrote the manuscript with input from all other authors. NW edited the manuscript. All authors proofread the manuscript.

Competing Interests Statement:

The authors have no conflict of interest to declare.

REFERENCE

1. Graw, J. Eye Development. *Curr. Top. Dev. Biol.* **90,** 343–386 (2010).
2. Heavner, W. & Pevny, L. Eye development and retinogenesis. *Cold Spring Harb. Perspect. Biol.* **4,** (2012).
3. Helga Kolb. Gross Anatomy of the Eye. *Webvision* (2012). Available at: http://webvision.med.utah.edu/book/part-i-foundations/gross-anatomy-of-the-ey/. (Accessed: 18th June 2018)
4. Masland, R. H. The Neuronal Organization of the Retina. *Neuron* **76,** 266–280 (2012).
5. Gawad, C., Koh, W. & Quake, S. R. Single-cell genome sequencing: current state of the science. *Nat. Rev. Genet.* **17,** 175–188 (2016).
6. Shekhar, K. *et al.* Comprehensive Classification of Retinal Bipolar Neurons by Single-Cell Transcriptomics. *Cell* **166,** 1308–1323.e30 (2016).
7. Macosko, E. Z. *et al.* Highly Parallel Genome-wide Expression Profiling of Individual Cells Using Nanoliter Droplets. *Cell* **161,** 1202–1214 (2015).
8. Rheaume, B. A. *et al.* Single cell transcriptome profiling of retinal ganglion cells identifies cellular subtypes. *Nat. Commun.* **9,** 2759 (2018).
9. Marmorstein, A. D. & Marmorstein, L. Y. The challenge of modeling macular degeneration in mice. *Trends Genet.* **23,** 225–231 (2007).
10. GREGORY S. HAGEMAN, KAREN GAEHRS, L. V. J. A. D. A. Age-Related Macular Degeneration (AMD). *Webvision.* Available at: https://webvision.med.utah.edu/book/part-xii-cell-biology-of-retinal-degenerations/age-related-macular-degeneration-amd/. (Accessed: 11th November 2018)
11. HELGA KOLB. Simple Anatomy of the Retina. *Webvision* Available at: https://webvision.med.utah.edu/book/part-i-foundations/simple-anatomy-of-the-retina/. (Accessed: 11th November 2018)

12. Li, M. *et al.* Comprehensive analysis of gene expression in human retina and supporting tissues. *Hum. Mol. Genet.* **23,** 4001–4014 (2014).

13. Sharon, D., Blackshaw, S., Cepko, C. L. & Dryja, T. P. Profile of the genes expressed in the human peripheral retina, macula, and retinal pigment epithelium determined through serial analysis of gene expression (SAGE). *Proc. Natl. Acad. Sci. U. S. A.* **99,** 315–20 (2002).

14. Fu, Y. *Phototransduction in Rods and Cones*. *Webvision: The Organization of the Retina and Visual System* (University of Utah Health Sciences Center, 1995).

15. Cepko, C. L. The Determination of Rod and Cone Photoreceptor Fate. *Annu. Rev. Vis. Sci.* **1,** 211–234 (2015).

16. HELGA KOLB. Cone Pathways through the Retina. *Webvision* Available at: https://webvision.med.utah.edu/book/part-iii-retinal-circuits/cone-pathways-through-the-retina/. (Accessed: 11th November 2018)

17. Hamel, C. P. Cone rod dystrophies. *Orphanet J. Rare Dis.* **2,** 7 (2007).

18. Michaelides, M., Hardcastle, A. J., Hunt, D. M. & Moore, A. T. Progressive Cone and Cone-Rod Dystrophies: Phenotypes and Underlying Molecular Genetic Basis. *Surv. Ophthalmol.* **51,** 232–258 (2006).

19. Zaneveld, S. A. *et al.* Gene Therapy Rescues Retinal Degeneration in Receptor Expression-Enhancing Protein 6 Mutant Mice. *Hum. Gene Ther.* hum.2018.078 (2018). doi:10.1089/hum.2018.078

20. Xue, K. *et al.* Beneficial effects on vision in patients undergoing retinal gene therapy for choroideremia. *Nat. Med.* **24,** 1507–1512 (2018).

21. Mukherjee, S. *et al.* CDK5 Inhibition Resolves PKA/cAMP-Independent Activation of CREB1 Signaling in Glioma Stem Cells. *Cell Rep.* **23,** 1651–1664 (2018).

22. Bosco, A. *et al.* Complement C3-Targeted Gene Therapy Restricts Onset and Progression of Neurodegeneration in Chronic Mouse Glaucoma. *Mol. Ther.* **26,** 2379–2396 (2018).

23. Osborne, A. *et al.* Neuroprotection of retinal ganglion cells by a novel gene therapy construct that achieves sustained enhancement of brain-derived neurotrophic factor/tropomyosin-related kinase receptor-B signaling. *Cell Death Dis.* **9,** 1007 (2018).

24. Simpson, E. M. *et al.* New MiniPromoter Ple345 (*NEFL*) Drives Strong and Specific Expression in Retinal Ganglion Cells of Mouse and Primate Retina. *Hum. Gene Ther.* hum.2018.118 (2018). doi:10.1089/hum.2018.118

25. Lacar, B. *et al.* Nuclear RNA-seq of single neurons reveals molecular signatures of activation. *Nat. Commun.* **7,** 11022 (2016).

26. Hu, P. *et al.* Dissecting Cell-Type Composition and Activity-Dependent Transcriptional State in Mammalian Brains by Massively Parallel Single-Nucleus RNA-Seq. *Mol. Cell* **68,** 1006–1015.e7 (2017).

27. Habib, N. *et al.* Massively parallel single-nucleus RNA-seq with DroNc-seq. *Nat. Methods* **14,** 955–958 (2017).

28. Lake, B. B. *et al.* Neuronal subtypes and diversity revealed by single-nucleus RNA sequencing of the human brain. *Science* **352,** 1586–90 (2016).

29. Morgan, D. J. & DeAngelis, M. M. Differential Gene Expression in Age-Related Macular Degeneration. *Cold Spring Harb. Perspect. Med.* **5,** a017210 (2014).

30. Dobin, A. *et al.* STAR: ultrafast universal RNA-seq aligner. *Bioinformatics* **29,** 15–21 (2013).

31. Trapnell, C. *et al.* Differential analysis of gene regulation at transcript resolution with RNA-seq. *Nat. Biotechnol.* **31,** 46–53 (2013).

32. Roberts, A., Pimentel, H., Trapnell, C. & Pachter, L. Identification of novel transcripts in annotated genomes using RNA-Seq. *Bioinformatics* **27,** 2325–2329 (2011).

33. Roberts, A., Trapnell, C., Donaghey, J., Rinn, J. L. & Pachter, L. Improving RNA-Seq expression estimates by correcting for fragment bias. *Genome Biol.* **12,** R22

(2011).

34. Trapnell, C. *et al.* Transcript assembly and quantification by RNA-Seq reveals unannotated transcripts and isoform switching during cell differentiation. *Nat. Biotechnol.* **28,** 511–515 (2010).

35. Anders, S., Pyl, P. T. & Huber, W. HTSeq--a Python framework to work with high-throughput sequencing data. *Bioinformatics* **31,** 166–9 (2015).

36. Butler, A., Hoffman, P., Smibert, P., Papalexi, E. & Satija, R. Integrating single-cell transcriptomic data across different conditions, technologies, and species. *Nat. Biotechnol.* **36,** 411–420 (2018).

37. Huang, D. *et al.* The DAVID Gene Functional Classification Tool: a novel biological module-centric algorithm to functionally analyze large gene lists. *Genome Biol.* **8,** R183 (2007).

38. DeAngelis, M. M. *et al.* Genetics of age-related macular degeneration (AMD). *Hum. Mol. Genet.* **26,** R246–R246 (2017).

39. Martin, P. R. & Grünert, U. Spatial density and immunoreactivity of bipolar cells in the macaque monkey retina. *J. Comp. Neurol.* **323,** 269–287 (1992).

40. Bringmann, A. *et al.* The primate fovea: Structure, function and development. *Prog. Retin. Eye Res.* **66,** 49–84 (2018).

41. Ortín-Martínez, A. *et al.* Number and Distribution of Mouse Retinal Cone Photoreceptors: Differences between an Albino (Swiss) and a Pigmented (C57/BL6) Strain. *PLoS One* **9,** e102392 (2014).

42. Hameed, A. *et al.* Evidence of RPGRIP1 gene mutations associated with recessive cone-rod dystrophy. *J. Med. Genet.* **40,** 616–9 (2003).

43. Dryja, T. P. *et al.* Null RPGRIP1 Alleles in Patients with Leber Congenital Amaurosis. *Am. J. Hum. Genet.* **68,** 1295–1298 (2001).

44. Kuznetsova, T. *et al.* Exclusion of *RPGRIP1* ins44 from Primary Causal Association with Early-Onset Cone–Rod Dystrophy in Dogs. *Investig.*

Opthalmology Vis. Sci. **53,** 5486 (2012).

45. Mavlyutov, T. A., Zhao, H. & Ferreira, P. A. Species-specific subcellular localization of RPGR and RPGRIP isoforms: implications for the phenotypic variability of congenital retinopathies among species. *Hum. Mol. Genet.* **11,** 1899–907 (2002).

46. Mellersh, C. S. *et al.* Canine RPGRIP1 mutation establishes cone–rod dystrophy in miniature longhaired dachshunds as a homologue of human Leber congenital amaurosis. *Genomics* **88,** 293–301 (2006).

47. Hanein, S. *et al.* Leber congenital amaurosis: Comprehensive survey of the genetic heterogeneity, refinement of the clinical definition, and genotype-phenotype correlations as a strategy for molecular diagnosis. *Hum. Mutat.* **23,** 306–317 (2004).

48. Roepman, R. *et al.* The retinitis pigmentosa GTPase regulator (RPGR) interacts with novel transport-like proteins in the outer segments of rod photoreceptors. *Hum. Mol. Genet.* **9,** 2095–105 (2000).

49. Boylan, J. P. & Wright, A. F. Identification of a novel protein interacting with RPGR. *Hum. Mol. Genet.* **9,** 2085–93 (2000).

50. Friedman, J. S. *et al.* Premature Truncation of a Novel Protein, RD3, Exhibiting Subnuclear Localization Is Associated with Retinal Degeneration. *Am. J. Hum. Genet.* **79,** 1059–1070 (2006).

51. Chang, B., Heckenlively, J. R., Hawes, N. L. & Roderick, T. H. New Mouse Primary Retinal Degeneration (rd-3). *Genomics* **16,** 45–49 (1993).

52. Zhao, Y. *et al.* The retinitis pigmentosa GTPase regulator (RPGR)- interacting protein: Subserving RPGR function and participating in disk morphogenesis. *Proc. Natl. Acad. Sci.* **100,** 3965–3970 (2003).

53. Won, J. *et al.* RPGRIP1 is essential for normal rod photoreceptor outer segment elaboration and morphogenesis. *Hum. Mol. Genet.* **18,** 4329–4339 (2009).

54. Ferrari, S. *et al.* Retinitis pigmentosa: genes and disease mechanisms. *Curr. Genomics* **12,** 238–49 (2011).

55. Zobor, D. & Zrenner, E. Retinitis pigmentosa – eine Übersicht. *Der Ophthalmol.* **109,** 501–515 (2012).

56. Goodwin, P. Hereditary retinal disease. *Curr. Opin. Ophthalmol.* **19,** 255–262 (2008).

57. Zhao, L. *et al.* Integrative subcellular proteomic analysis allows accurate prediction of human disease-causing genes. *Genome Res.* **26,** 660–669 (2016).

58. Kolesnikov, A. V *et al.* G-protein betagamma-complex is crucial for efficient signal amplification in vision. *J. Neurosci.* **31,** 8067–77 (2011).

59. Maeda, A. *et al.* Role of photoreceptor-specific retinol dehydrogenase in the retinoid cycle in vivo. *J. Biol. Chem.* **280,** 18822–32 (2005).

60. Matsubara, S., Yamaji, Y., Sato, M., Fujita, J. & Takahara, J. Expression of a photoreceptor protein, recoverin, as a cancer-associated retinopathy autoantigen in human lung cancer cell lines. *Br. J. Cancer* **74,** 1419–22 (1996).

61. Xie, Y. (Angela) *et al.* New syndrome with retinitis pigmentosa is caused by nonsense mutations in retinol dehydrogenase RDH11. *Hum. Mol. Genet.* **23,** 5774–5780 (2014).

62. van Genderen, M. M. *et al.* Mutations in TRPM1 Are a Common Cause of Complete Congenital Stationary Night Blindness. *Am. J. Hum. Genet.* **85,** 730–736 (2009).

63. Li, Z. *et al.* Recessive Mutations of the Gene TRPM1 Abrogate ON Bipolar Cell Function and Cause Complete Congenital Stationary Night Blindness in Humans. *Am. J. Hum. Genet.* **85,** 711–719 (2009).

64. Bellone, R. R. *et al.* Differential Gene Expression of TRPM1, the Potential Cause of Congenital Stationary Night Blindness and Coat Spotting Patterns (LP) in the Appaloosa Horse (Equus caballus). *Genetics* **179,** 1861–1870 (2008).

65. Audo, I. *et al.* TRPM1 Is Mutated in Patients with Autosomal-Recessive Complete Congenital Stationary Night Blindness. *Am. J. Hum. Genet.* **85,** 720–729 (2009).

66. Zeitz, C. *et al.* Mutations in *GRM6* Cause Autosomal Recessive Congenital Stationary Night Blindness with a Distinctive Scotopic 15-Hz Flicker Electroretinogram. *Investig. Opthalmology Vis. Sci.* **46,** 4328 (2005).

67. Dryja, T. P. *et al.* Night blindness and abnormal cone electroretinogram ON responses in patients with mutations in the GRM6 gene encoding mGluR6. *Proc. Natl. Acad. Sci.* **102,** 4884–4889 (2005).

68. Masu, M. *et al.* Specific deficit of the ON response in visual transmission by targeted disruption of the mGluR6 gene. *Cell* **80,** 757–65 (1995).

69. Gao, R. *et al.* Nanogrid single-nucleus RNA sequencing reveals phenotypic diversity in breast cancer. *Nat. Commun.* **8,** 228 (2017).

70. Mustafi, D. *et al.* Transcriptome analysis reveals rod/cone photoreceptor specific signatures across mammalian retinas. *Hum. Mol. Genet.* **25,** ddw268 (2016).

71. Welby, E. *et al.* Isolation and Comparative Transcriptome Analysis of Human Fetal and iPSC-Derived Cone Photoreceptor Cells. *Stem Cell Reports* **9,** 1898–1915 (2017).

FIGURE LEGENDS:

Table1. Basic sample information showing nuclei numbers and correlation with bulk RNA-seq of the same sample.

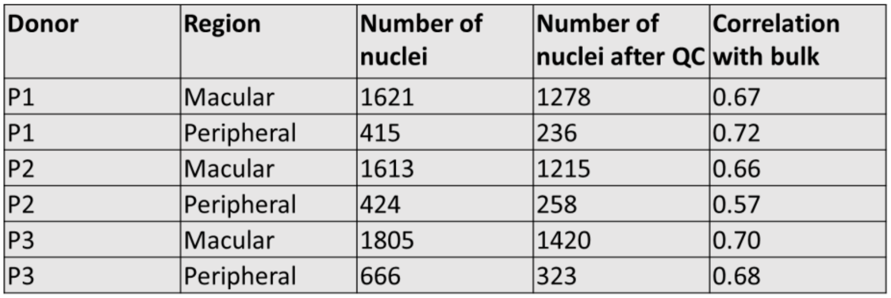

Donor	Region	Number of nuclei	Number of nuclei after QC	Correlation with bulk
P1	Macular	1621	1278	0.67
P1	Peripheral	415	236	0.72
P2	Macular	1613	1215	0.66
P2	Peripheral	424	258	0.57
P3	Macular	1805	1420	0.70
P3	Peripheral	666	323	0.68

Figure 1. Unsupervised clustering identifies 7 major cell types in human retina.

A. Clustering of 4730 human retina single nuclei expression profiles into 7 populations (left) and representation of alignment of 6 dataset from 3 donors.

B. Heatmap of top 15 DEGs in each cell type.

C. Profiles of known markers (PDE6A, GRM6, SLC1A3, GAD1, SEPT4, ARR3, RBPMS) in each cluster.

D. Proportion of 7 major cell types in macular and peripheral region of human retina.

E. Comparison of proportion of 7 major cell types of mouse and human retina.

Figure 2. Differentially expressed genes are revealed in rod and cone photoreceptors.

A. Biological process GO term enrichment by photoreceptor cell DEGs

B. Biological process GO term enrichment by genes showing higher expression in rod cells than cone cells.

C. Biological process GO term enrichment by genes showing higher expression in cone cells than rod cells.

D. Intersection of human and mouse photoreceptor DEGs

E. Demonstration of two genes that show different distribution in human and mouse photoreceptors.

Figure 3. Transcriptome difference revealed between macular and peripheral region.

A. Biological process GO term enrichment by genes showing higher expression in macular cells than peripheral cells.

B. Biological process GO term enrichment by genes showing higher expression in peripheral cells than macular cells.

C. Heatmap demonstrating correlation of averaged gene expression of five major cell types in six samples.

Figure 4. Photoreceptor DEGs enrich human IRDs.

A. IRD genes generally show higher expression level than the rest of genes in human retina.

B. Distribution of human retinal disease genes, mouse eye phenotype genes (but no human disease discovered), mouse retinal expressing genes (but no eye phenotype found) in DEGs of all cell types (PR is merged from rod and cone).

C. RP genes and CRD genes show different expression pattern in rod and cone photoreceptors.

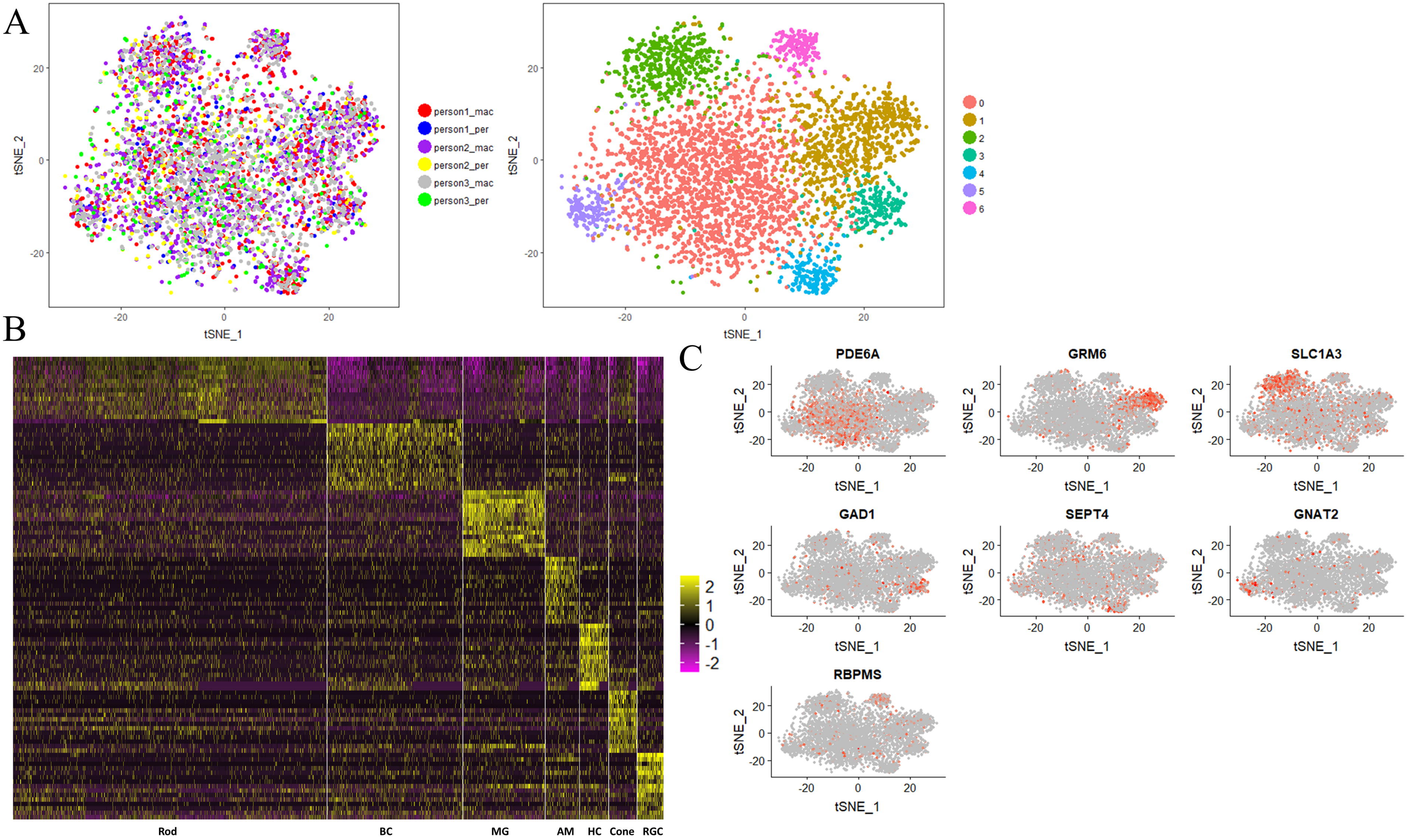

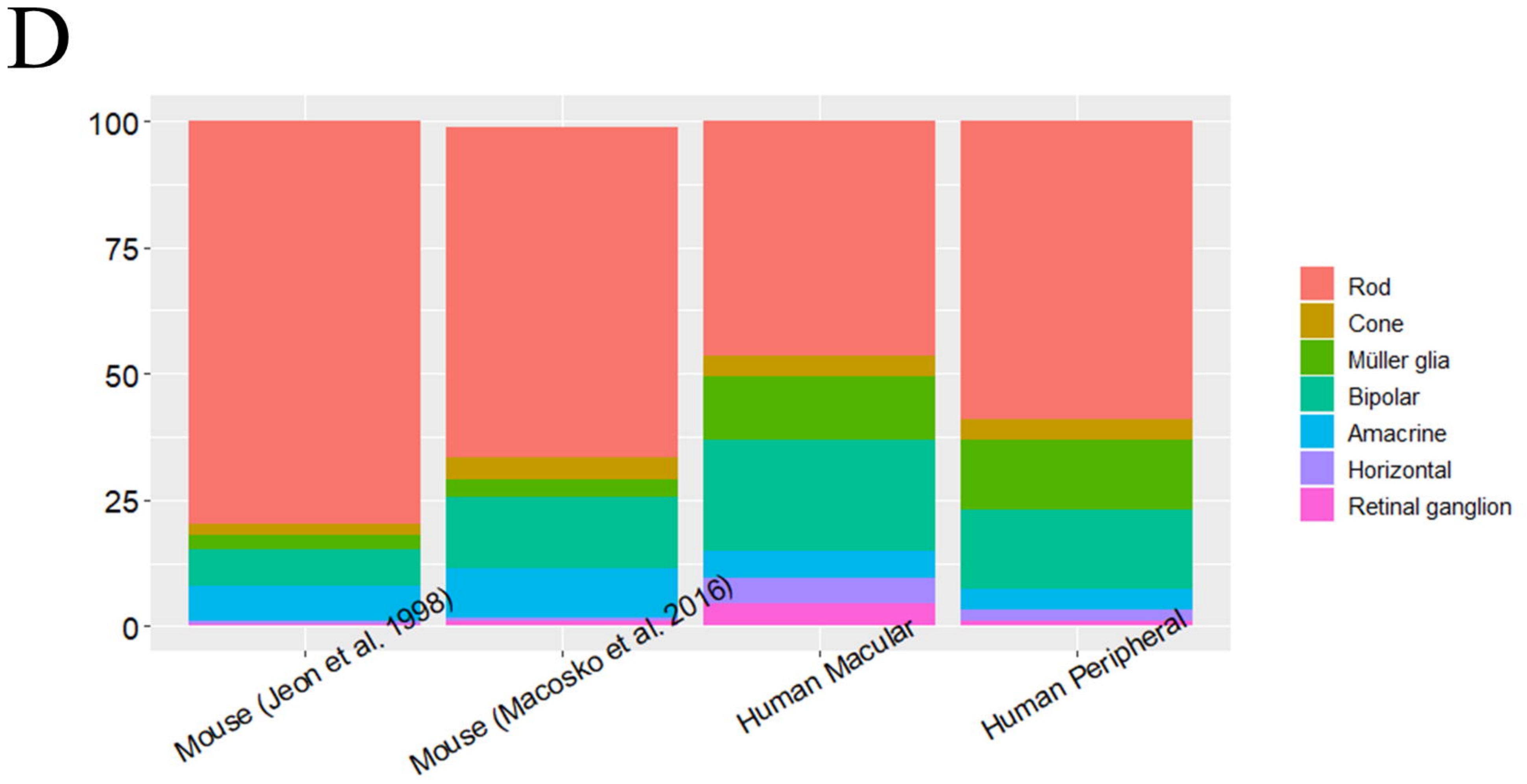

E

Cell type	Mouse retinal cell proportion (%) (Jeon et al. 1998)	Mouse retinal cell proportion (%) (Macosko et al. 2016)	Human macular cell proportion (%)	Human peripheral cell proportion (%)
Rod	79.9	65.6	46.31	59.13
Cone	2.1	4.2	4.32	4.16
MG	2.8	3.6	12.39	13.83
BC	7.3	14.0	22.03	15.67
AM	7.0	9.9	5.39	4.16
HC	0.5	0.6	4.93	1.96
RGC	0.5	1.0	4.63	1.10

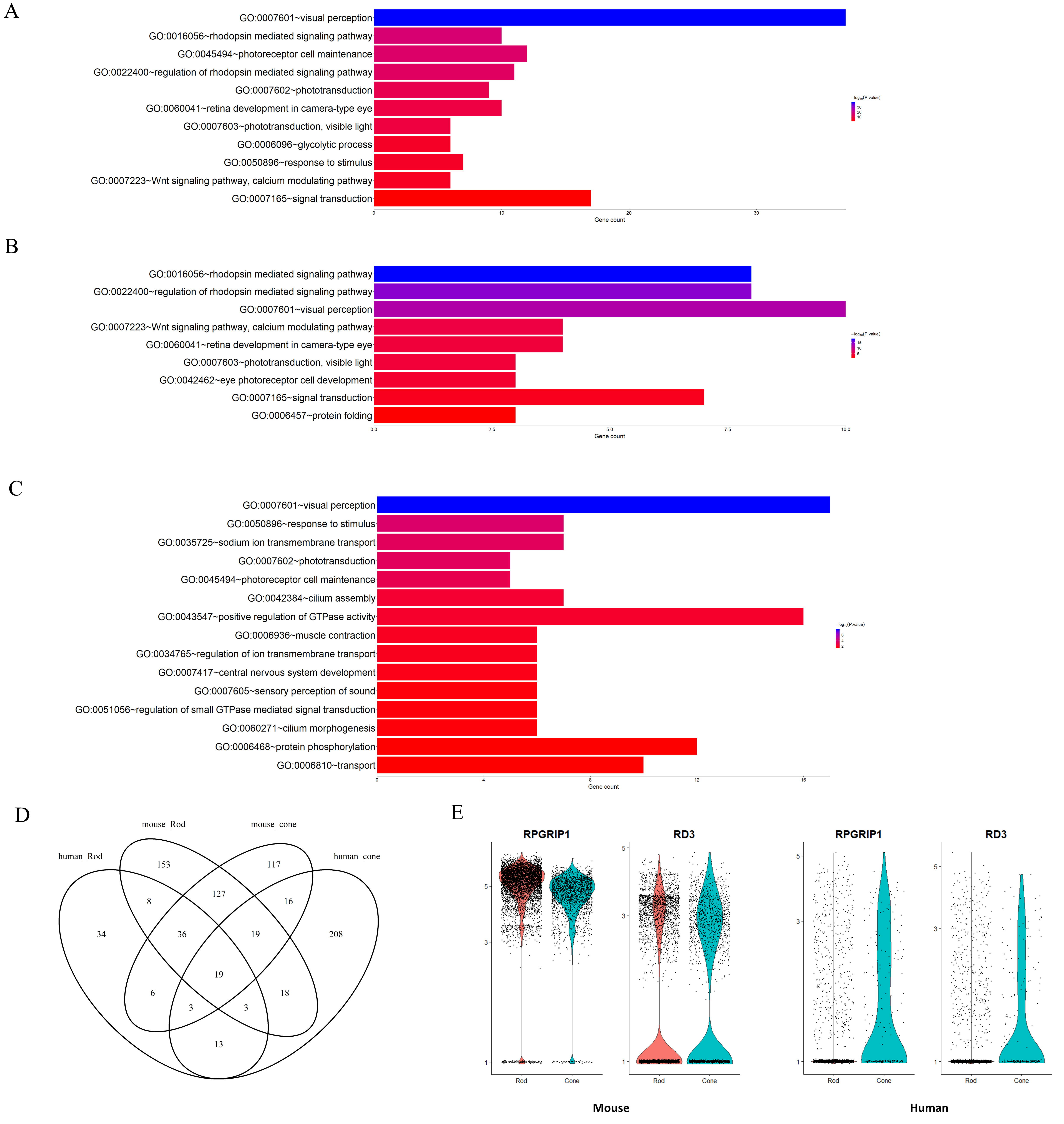
A
GO:0007601~visual perception
GO:0016056~rhodopsin mediated signaling pathway
GO:0045494~photoreceptor cell maintenance
GO:0022400~regulation of rhodopsin mediated signaling pathway
GO:0007602~phototransduction
GO:0060041~retina development in camera-type eye
GO:0007603~phototransduction, visible light
GO:0006096~glycolytic process
GO:0050896~response to stimulus
GO:0007223~Wnt signaling pathway, calcium modulating pathway
GO:0007165~signal transduction
0
10
20
30
Gene count
$-\log_{10}$(P.value)
30
20
10
B
GO:0016056~rhodopsin mediated signaling pathway
GO:0022400~regulation of rhodopsin mediated signaling pathway
GO:0007601~visual perception
GO:0007223~Wnt signaling pathway, calcium modulating pathway
GO:0060041~retina development in camera-type eye
GO:0007603~phototransduction, visible light
GO:0042462~eye photoreceptor cell development
GO:0007165~signal transduction
GO:0006457~protein folding
0.0
2.5
5.0
7.5
10.0
Gene count
$-\log_{10}$(P.value)
15
10
5
C
GO:0007601~visual perception
GO:0050896~response to stimulus
GO:0035725~sodium ion transmembrane transport
GO:0007602~phototransduction
GO:0045494~photoreceptor cell maintenance
GO:0042384~cilium assembly
GO:0043547~positive regulation of GTPase activity
GO:0006936~muscle contraction
GO:0034765~regulation of ion transmembrane transport
GO:0007417~central nervous system development
GO:0007605~sensory perception of sound
GO:0051056~regulation of small GTPase mediated signal transduction
GO:0060271~cilium morphogenesis
GO:0006468~protein phosphorylation
GO:0006810~transport
0
4
8
12
16
Gene count
$-\log_{10}$(P.value)
6
4
2
D
mouse_Rod
mouse_cone
human_Rod
human_cone
153
117
8
127
16
34
36
19
208
19
6
18
3
3
13
E
RPGRIP1
RD3
RPGRIP1
RD3
5
3
1
Rod
Cone
Mouse
Human

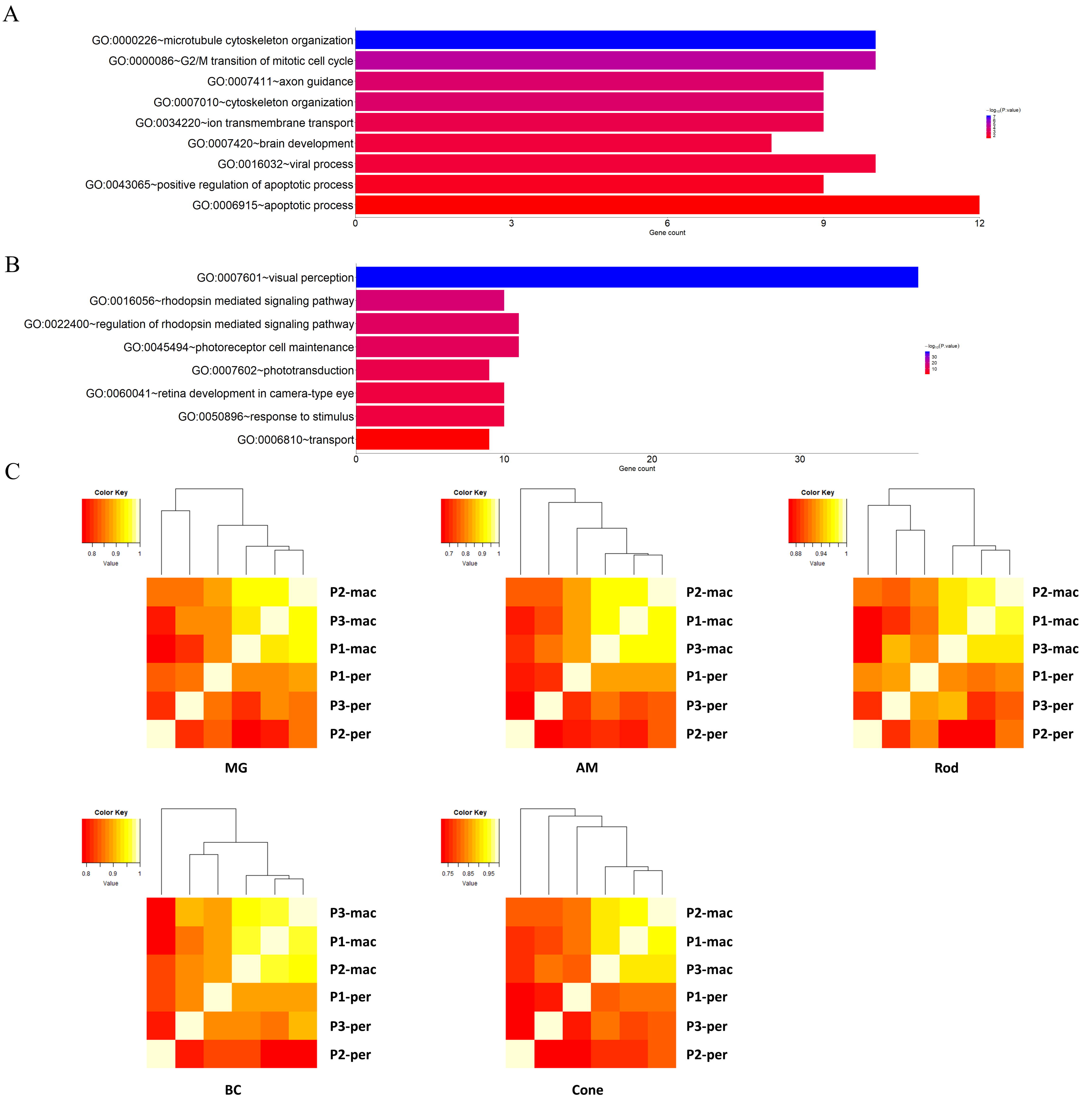
A
GO:0000226~microtubule cytoskeleton organization
GO:0000086~G2/M transition of mitotic cell cycle
GO:0007411~axon guidance
GO:0007010~cytoskeleton organization
GO:0034220~ion transmembrane transport
GO:0007420~brain development
GO:0016032~viral process
GO:0043065~positive regulation of apoptotic process
GO:0006915~apoptotic process
0
3
6
9
12
Gene count
$-\log_{10}$(P.value)
7
6
5
4
3
2
B
GO:0007601~visual perception
GO:0016056~rhodopsin mediated signaling pathway
GO:0022400~regulation of rhodopsin mediated signaling pathway
GO:0045494~photoreceptor cell maintenance
GO:0007602~phototransduction
GO:0060041~retina development in camera-type eye
GO:0050896~response to stimulus
GO:0006810~transport
0
10
20
30
Gene count
$-\log_{10}$(P.value)
30
20
10
C
Color Key
0.8
0.9
1
Value
P2-mac
P3-mac
P1-mac
P1-per
P3-per
P2-per
MG
Color Key
0.7
0.8
0.9
1
Value
P2-mac
P1-mac
P3-mac
P1-per
P3-per
P2-per
AM
Color Key
0.88
0.94
1
Value
P2-mac
P1-mac
P3-mac
P1-per
P3-per
P2-per
Rod
Color Key
0.8
0.9
1
Value
P3-mac
P1-mac
P2-mac
P1-per
P3-per
P2-per
BC
Color Key
0.75
0.85
0.95
Value
P2-mac
P1-mac
P3-mac
P1-per
P3-per
P2-per
Cone

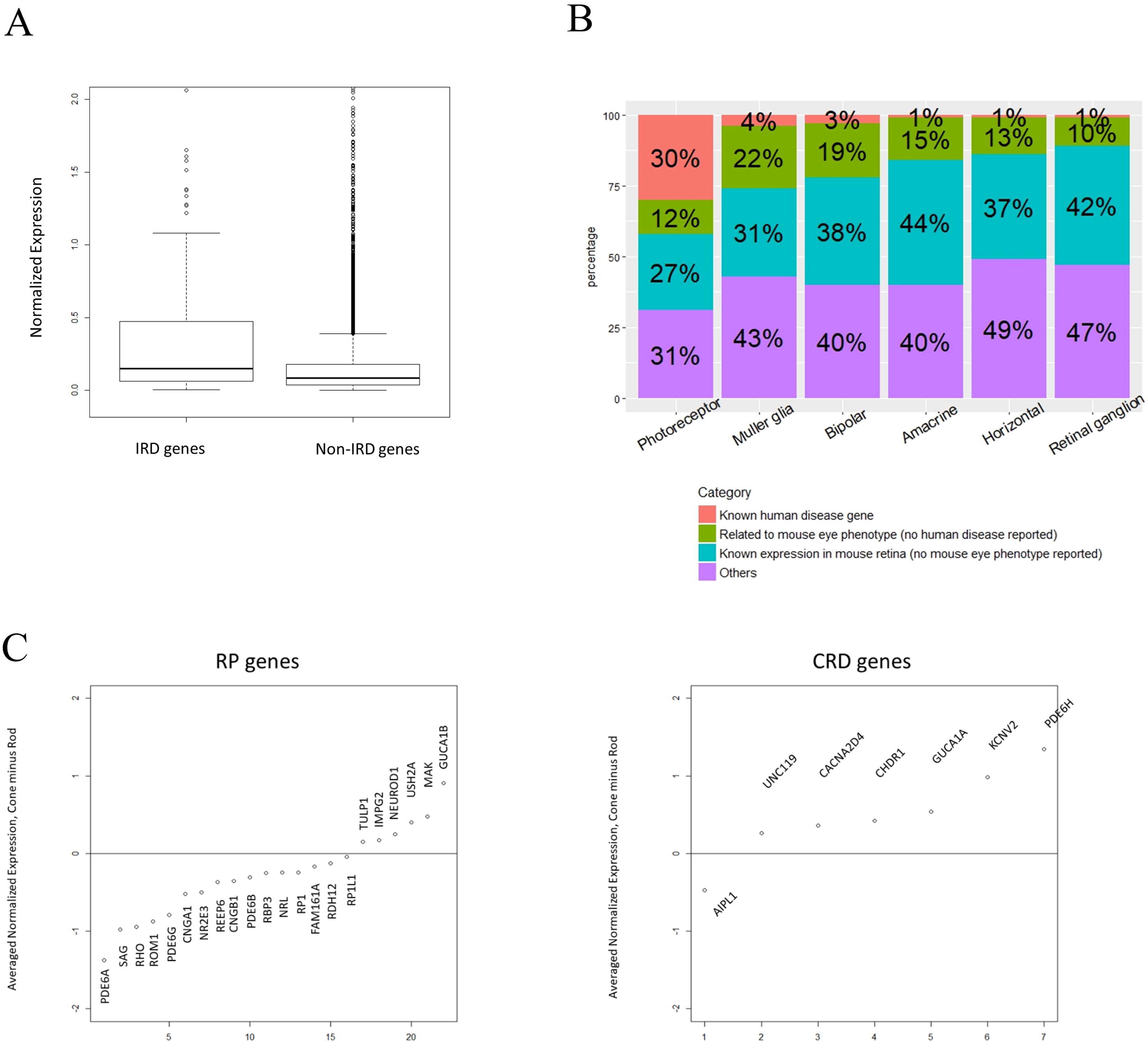
A
Normalized Expression
0.0
0.5
1.0
1.5
2.0
IRD genes
Non-IRD genes
B
percentage
0
25
50
75
100
30%
12%
27%
31%
4%
22%
31%
43%
3%
19%
38%
40%
1%
15%
44%
40%
1%
13%
37%
49%
1%
10%
42%
47%
Photoreceptor
Muller glia
Bipolar
Amacrine
Horizontal
Retinal ganglion
Category
Known human disease gene
Related to mouse eye phenotype (no human disease reported)
Known expression in mouse retina (no mouse eye phenotype reported)
Others
C
RP genes
Averaged Normalized Expression, Cone minus Rod
-2
-1
0
1
2
5
10
15
20
PDE6A
SAG
RHO
ROM1
PDE6G
CNGA1
NR2E3
REEP6
CNGB1
PDE6B
RBP3
NRL
RP1
FAM161A
RDH12
RP1L1
TULP1
IMPG2
NEUROD1
USH2A
MAK
GUCA1B
CRD genes
Averaged Normalized Expression, Cone minus Rod
-2
-1
0
1
2
1
2
3
4
5
6
7
AIPL1
UNC119
CACNA2D4
CHDR1
GUCA1A
KCNV2
PDE6H